Estimadores Espectrais Suavizados

O periodograma não é um bom estimador do espectro, dada a sua grande instabilidade.

Obter estimadores espectrais que têm propriedades melhores do que o periodograma.

Dois métodos para obter estimadores mais estáveis, ambos conduzindo aos chamados estimadores espectrais suavizados (estimador não paramétrico):

- O processo de suavização no tempo e depois transformar para o domínio de frequências, obtendo os estimadores suavizados de covariâncias.
- O processo de suavização é feito no próprio domínio de frequências e teremos os estimadores suavizados de periodogramas.

Em ambos os casos, obtemos estimadores que são assintoticamente não viesados e com variâncias que decrescem com o número de observações da série temporal.

Além desses dois métodos, há um método de estimador paramétrico.

O processo de suavização no tempo e depois transformar para o domínio de frequências, obtendo os estimadores suavizados de covariâncias.

Transformada discreta de Fourier

$$d_\nu^{(T)} = \frac{1}{\sqrt{2\pi T}} \sum_{t=1}^{T} X_t e^{-i2\pi\nu t/T}. \tag{8.2}$$

Periodograma:

$$I_\nu^{(T)} = |d_\nu^{(T)}|^2 = \frac{1}{2\pi T} \left| \sum_{t=1}^{T} X_t e^{-i\lambda_\nu t} \right|^2, \tag{8.8}$$

para frequências $\lambda_\nu = (2\pi\nu)/T$, $-[(T-1)/2] \leq \nu \leq [T/2]$. Podemos, também, definir o periodograma para qualquer frequência $\lambda \in [-\pi, \pi]$, ou seja,

$$I^{(T)}(\lambda) = |d^{(T)}(\lambda)|^2, \tag{8.9}$$

Como o espectro é definido por

$$f(\lambda) = \frac{1}{2\pi} \sum_{\tau=-\infty}^{\infty} e^{-i\lambda\tau}\gamma_\tau, \quad -\pi \leq \lambda \leq \pi,$$

a idéia natural é substituir γ_τ por um estimador.

Suponha, então, que tenhamos observações $X_1, \ldots, X_T$ do processo estacionário X_t e estimamos γ_k por

$$c_k = \begin{cases} \frac{1}{T}\sum_{t=1}^{T-|k|}\{X_t - \overline{X}\}\{X_{t+|k|} - \overline{X}\}, & \text{se } |k| \leq T-1 \\ 0, & \text{se } |k| > T-1, \end{cases} \tag{8.18}$$

onde $\overline{X}$ é a *média amostral*

$$\overline{X} = \frac{1}{T}\sum_{t=1}^{T} X_t.$$

Sem perda de generalidade, vamos supor que a média do processo seja zero, de modo que $\overline{X}$ é omitida em (8.18) e obtemos

$$E\{c_k\} = \frac{1}{T}\sum_{t=1}^{T-|k|} E\{X_t X_{t+|k|}\}$$

$$= \frac{1}{T}\sum_{t=1}^{T-|k|}\gamma_k = (1-\frac{|k|}{T})\gamma_k, \tag{8.19}$$

o que mostra que c_k é viesado. Se, em (8.18), colocarmos $T-|k|$ no denominador, no lugar de T, obteremos um estimador não viesado de γ_k. Contudo, o estimador definido por (8.18) tem um erro quadrático médio menor que o estimador não viesado. De (8.19), vemos que c_k é assintoticamente não viesado.

Se a média do processo não for zero não é difícil verificar, de (8.18), que

$$c_k = \frac{1}{T}\sum_{t=1}^{T-|k|}[X_t-\mu][X_{t+|k|}-\mu] - (1-\frac{|k|}{T})(\overline{X}-\mu)^2, \tag{8.20}$$

de modo que

$$E\{c_k\} = (1-\frac{|k|}{T})\gamma_k - (1-\frac{|k|}{T})\mathrm{Var}(\overline{X}). \tag{8.21}$$

Por outro lado (Morettin, 1979, p. 152),

$$\mathrm{Var}(\overline{X}) = \frac{1}{T}\sum_{k=-T}^{T}(1-\frac{|k|}{T})\gamma_k,$$

de modo que se a média do processo não for zero, vemos de (8.21) que o viés do estimador é acrescido de um termo de $O(T^{-1})$.

Estimando-se $f(\lambda)$ por

$$\hat{f}(\lambda) = \frac{1}{2\pi}\sum_{k=-\infty}^{\infty}e^{-i\lambda k}c_k, \tag{8.22}$$

é fácil notar que esse estimador coincide com $I^{(T)}(\lambda)$. Vamos usar (8.22) para obter estimadores mais estáveis do que o periodograma.

Observamos que

$$E\{I^{(T)}(\lambda)\} = (2\pi)^{-1} \sum_{\tau=-T+1}^{T-1} (1 - \frac{|\tau|}{T})\gamma_\tau e^{-i\lambda\tau}. \tag{8.23}$$

Chamando

$$w(\tau) = \begin{cases} 1 - \frac{|\tau|}{T}, & \text{se } |\tau| \leq T-1 \\ 0, & \text{se } |\tau| > T-1, \end{cases} \tag{8.24}$$

vemos que (8.23) é a transformada de Fourier do produto $w(\tau)\gamma_\tau$; logo, temos

$$E\{I^{(T)}(\lambda)\} = \int_{-\pi}^{\pi} W(\alpha) f(\lambda - \alpha) d\alpha, \tag{8.25}$$

na qual $W(\lambda)$ é a transformada de Fourier de $w(\tau)$, dada por

$$W(\lambda) = T \left[\frac{\text{sen}(\pi T \lambda)}{\pi T \lambda} \right]^2. \tag{8.26}$$

A equação (8.25) nos diz que o periodograma tem um valor esperado que corresponde a "olhar o espectro através da janela $W(\lambda)$". Como, para T grande, $W(\lambda)$ comporta-se como uma função delta de Dirac, (8.25) também nos diz que $I^{(T)}(\lambda)$ é assintoticamente não viesado.

$$\hat{f}(\lambda) = \frac{1}{2\pi} \sum_{\tau=-\infty}^{\infty} w_M(\tau) c_\tau e^{-i\lambda\tau}, \quad -\pi \leq \lambda \leq \pi, \tag{8.29}$$

onde, para um inteiro $M < T$, $w_M(\tau)$, $\tau = 0, \pm 1, \ldots$, é uma sequência de pesos satisfazendo:

(i) $0 \leq w_M(\tau) \leq w_M(0) = 1$

(ii) $w_M(-\tau) = w_M(\tau)$, para todo τ

(iii) $w_M(\tau) = 0$, $|\tau| > M$.

O estimador $\hat{f}(\lambda)$ é chamado *estimador suavizado de covariâncias.* A *janela espectral* correspondente à função peso (núcleo) $w_M(\tau)$ é definida por

$$W_M(\lambda) = \frac{1}{2\pi} \sum_{\tau} e^{-i\lambda\tau} w_M(\tau). \tag{8.30}$$

Segue-se que $W_M(\lambda)$ satisfaz:

(i) $W_M(-\lambda) = W_M(\lambda)$, para todo λ;

(ii) $\int_{-\pi}^{\pi} W_M(\lambda)d\lambda = w_M(0) = 1$.

De (8.29), obtemos que $\hat{f}(\lambda)$ é a convolução das transformadas de Fourier de $w_M(\tau)$ e c_τ, isto é,

$$\hat{f}(\lambda) = \int_{-\pi}^{\pi} W_M(\lambda - \alpha) I^{(T)}(\alpha) d\alpha. \tag{8.31}$$

Tomando o valor esperado de (8.31), obtemos

$$\begin{aligned} E\{\hat{f}(\lambda)\} &= \int_{-\pi}^{\pi} W_M(\lambda - \alpha) E\{I^{(T)}(\alpha)\} d\alpha \\ &\approx \int_{-\pi}^{\pi} W_M(\lambda - \alpha) f(\alpha) d\alpha. \end{aligned} \tag{8.32}$$

Supondo a janela $W_M(\lambda)$ concentrada ao redor de $\lambda = 0$ e $f(\lambda)$ constante sobre todo intervalo de frequências de comprimento comparável com a largura do pico da janela, podemos escrever

$$E\{\hat{f}(\lambda)\} \approx f(\lambda) \int_{-\pi}^{\pi} W_M(\alpha) d\alpha. \tag{8.33}$$

Sob essas mesmas condições, pode-se provar que

$$Var\{\hat{f}(\lambda)\} \approx \frac{2\pi}{T} f^2(\lambda) \int_{-\pi}^{\pi} W_M^2(\alpha) d\alpha, \tag{8.34}$$

o que será feito adiante. A relação (8.34) vem do fato que

$$\begin{aligned} &\text{Cov}\{\hat{f}(\lambda_1), \hat{f}(\lambda_2)\} \approx \\ &\approx \frac{2\pi}{T} \int_{-\pi}^{\pi} W_M(\lambda_1 - \alpha)[W_M(\lambda_2 - \alpha) + W_M(\lambda_2 + \alpha)] f^2(\alpha) d\alpha, \end{aligned} \tag{8.35}$$

que por sua vez é obtida de (8.31) (Jenkins e Watts, 1968, p. 412). A relação (8.35) mostra que a covariância entre os estimadores espectrais suavizados de covariâncias depende da intersecção entre as janelas espectrais centradas em λ_1 e λ_2.

4.5 Nonparametric Spectral Estimation

To continue the discussion that ended the previous section, we introduce a frequency band, $\mathcal{B}$, of $L << n$ contiguous fundamental frequencies, centered around frequency $\omega_j = j/n$, which is chosen close to a frequency of interest, ω. For frequencies of the form $\omega^* = \omega_j + k/n$, let

$$\mathcal{B} = \left\{\omega^* : \ \omega_j - \frac{m}{n} \leq \omega^* \leq \omega_j + \frac{m}{n}\right\}, \tag{4.44}$$

where

$$L = 2m + 1 \tag{4.45}$$

is an odd number, chosen such that the spectral values in the interval $\mathcal{B}$,

$$f(\omega_j + k/n), \quad k = -m, \ldots, 0, \ldots, m$$

are approximately equal to $f(\omega)$. This structure can be realized for large sample sizes, as shown formally in §C.2.

We now define an averaged (or smoothed) periodogram as the average of the periodogram values, say,

$$\bar{f}(\omega) = \frac{1}{L}\sum_{k=-m}^{m} I(\omega_j + k/n), \tag{4.46}$$

over the band $\mathcal{B}$. Under the assumption that the spectral density is fairly constant in the band $\mathcal{B}$, and in view of (4.41) we can show that under appropriate conditions,[11] for large n, the periodograms in (4.46) are approximately distributed as independent $f(\omega)\chi^2_2/2$ random variables, for $0 < \omega < 1/2$, as long as we keep L fairly small relative to n. This result is discussed formally in §C.2. Thus, under these conditions, $L\bar{f}(\omega)$ is the sum of L approximately independent $f(\omega)\chi^2_2/2$ random variables. It follows that, for large n,

$$\frac{2L\bar{f}(\omega)}{f(\omega)} \dot{\sim} \chi^2_{2L} \tag{4.47}$$

where $\dot{\sim}$ means *is approximately distributed as.*

$$B_w = \frac{L}{n}, \tag{4.48}$$

the bandwidth.[12] The concept of the bandwidth, however, becomes more complicated with the introduction of spectral estimators that smooth with unequal weights. Note (4.48) implies the degrees of freedom can be expressed as

$$2L = 2B_w n, \tag{4.49}$$

or twice the time-bandwidth product. The result (4.47) can be rearranged to obtain an approximate $100(1-\alpha)\%$ confidence interval of the form

$$\frac{2L\bar{f}(\omega)}{\chi^2_{2L}(1-\alpha/2)} \leq f(\omega) \leq \frac{2L\bar{f}(\omega)}{\chi^2_{2L}(\alpha/2)} \tag{4.50}$$

for the true spectrum, $f(\omega)$.

Example 4.11 Averaged Periodogram for SOI and Recruitment

Generally, it is a good idea to try several bandwidths that seem to be compatible with the general overall shape of the spectrum, as suggested by the periodogram. The SOI and Recruitment series periodograms, previously computed in Figure 4.4, suggest the power in the lower El Niño frequency needs smoothing to identify the predominant overall period. Trying values of L leads to the choice $L = 9$ as a reasonable value, and the result is displayed in Figure 4.5. In our notation, the bandwidth in this case is $B_w = 9/480 = .01875$ cycles per month for the spectral estimator. This bandwidth means we are assuming a relatively constant spectrum over about $.01875/.5 = 3.75\%$ of the entire frequency interval $(0, 1/2)$. To obtain the bandwidth, $B_w = .01875$, from the one reported by R in Figure 4.5, we can multiply $.065\Delta$ (the frequency scale is in increments of Δ) by $\sqrt{12}$ as discussed in footnote 12 on page 197.

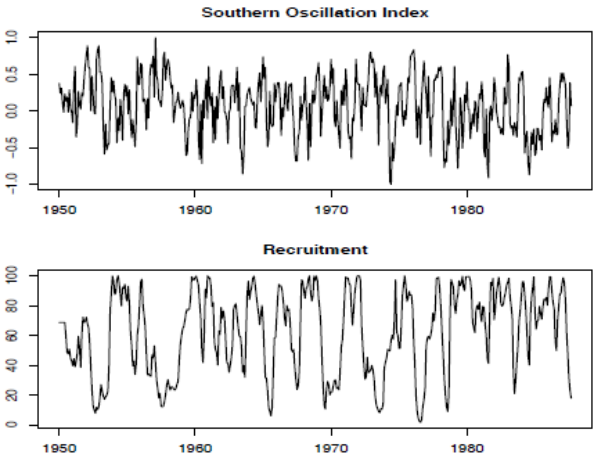

Fig. 1.5. Monthly SOI and Recruitment (estimated new fish), 1950-1987.

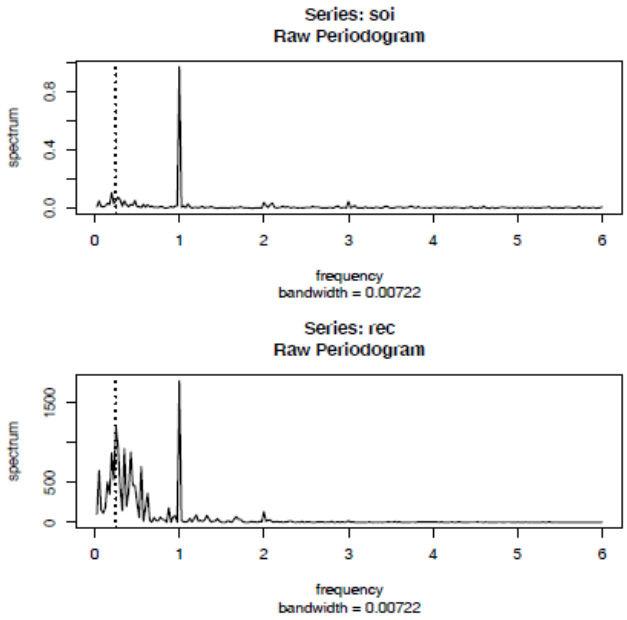

Fig. 4.4. Periodogram of SOI and Recruitment, $n = 453$ ($n' = 480$), where the frequency axis is labeled in multiples of $\Delta = 1/12$. Note the common peaks at $\omega = 1\Delta = 1/12$, or one cycle per year (12 months), and $\omega = \frac{1}{4}\Delta = 1/48$, or one cycle every four years (48 months).

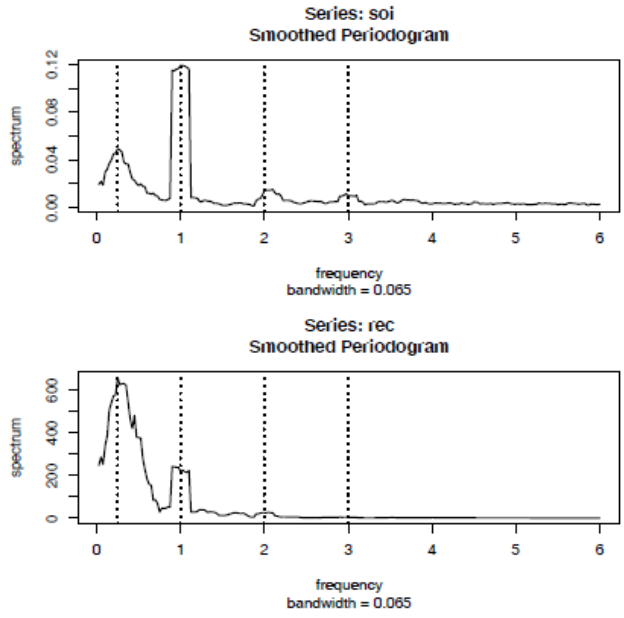

Fig. 4.5. The averaged periodogram of the SOI and Recruitment series $n = 453$, $n' = 480$, $L = 9$, $df = 17$, showing common peaks at the four year period, $\omega = \frac{1}{4}\Delta = 1/48$ cycles/month, the yearly period, $\omega = 1\Delta = 1/12$ cycles/month and some of its harmonics $\omega = k\Delta$ for $k = 2, 3$.

The adjusted degrees of freedom are $df = 2(9)(453)/480 \approx 17$. We can use this value for the 95% confidence intervals, with $\chi^2_{df}(.025) = 7.56$ and $\chi^2_{df}(.975) = 30.17$. Substituting into (4.53) gives the intervals in Table 4.1 for the two frequency bands identified as having the maximum power.

Table 4.1. Confidence Intervals for the Spectra of the SOI and Recruitment Series

Series	ω	Period	Power	Lower	Upper
SOI	1/48	4 years	.05	.03	.11
	1/12	1 year	.12	.07	.27
Recruits	1/48	4 years	6.59	3.71	14.82
$\times 10^2$	1/12	1 year	2.19	1.24	4.93

Many times, the visual impact of a spectral density plot will be improved by plotting the logarithm of the spectrum instead of the spectrum (the log transformation is the variance stabilizing transformation in this situation). This phenomenon can occur when regions of the spectrum exist with peaks of interest much smaller than some of the main power components. For the log spectrum, we obtain an interval of the form

$$\big[\log \bar{f}(\omega) + \log 2L - \log \chi^2_{2L}(1-\alpha/2), \quad \log \bar{f}(\omega) + \log 2L - \log \chi^2_{2L}(\alpha/2)\big]. \quad (4.51)$$

We can also test hypotheses relating to the equality of spectra using the fact that the distributional result (4.47) implies that the ratio of spectra based on roughly independent samples will have an approximate $F_{2L,2L}$ distribution. The independent estimators can either be from different frequency bands or from different series.

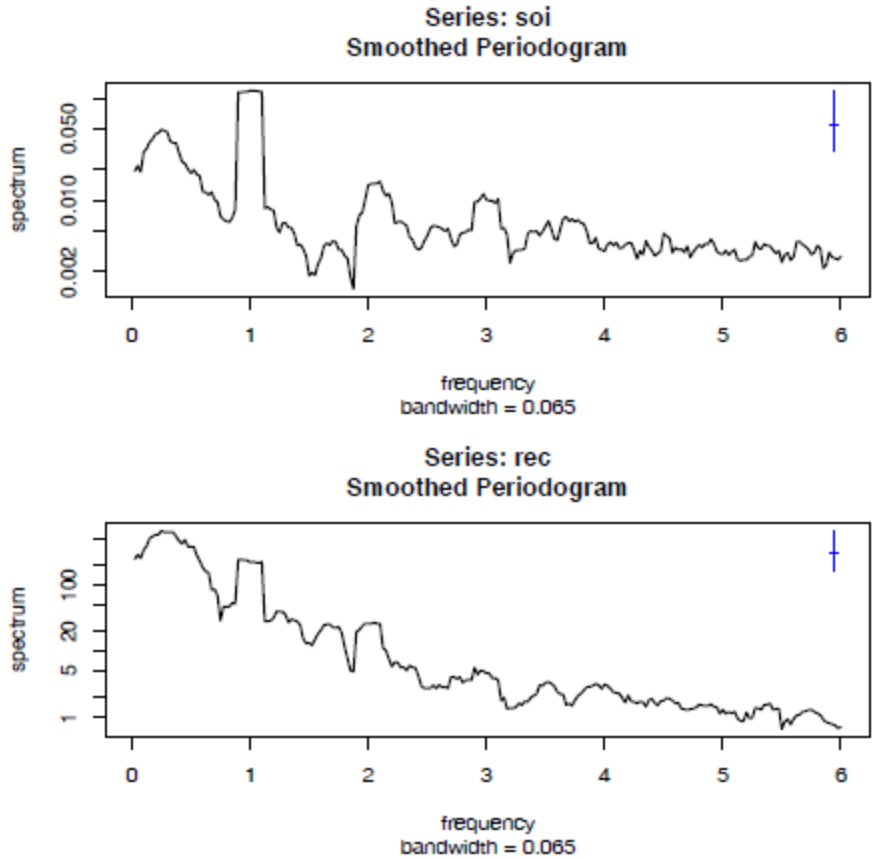

Fig. 4.6. Figure 4.5 with the average periodogram ordinates plotted on a $\log_{10}$ scale. The display in the upper right-hand corner represents a generic 95% confidence interval.

To address the problem of resolution, it should be evident that the flattening of the peaks in Figures 4.5 and 4.6 was due to the fact that simple averaging was used in computing $\bar{f}(\omega)$ defined in (4.46). There is no particular reason to use simple averaging, and we might improve the estimator by employing a weighted average, say

$$\widehat{f}(\omega) = \sum_{k=-m}^{m} h_k \, I(\omega_j + k/n), \tag{4.56}$$

using the same definitions as in (4.46) but where the weights $h_k > 0$ satisfy

$$\sum_{k=-m}^{m} h_k = 1.$$

In particular, it seems reasonable that the resolution of the estimator will improve if we use weights that decrease as distance from the center weight h_0 increases; we will return to this idea shortly. To obtain the averaged periodogram, $\bar{f}(\omega)$, in (4.56), set $h_k = L^{-1}$, for all k, where $L = 2m + 1$. The asymptotic theory established for $\bar{f}(\omega)$ still holds for $\widehat{f}(\omega)$ provided that the weights satisfy the additional condition that if $m \to \infty$ as $n \to \infty$ but $m/n \to 0$, then

$$\sum_{k=-m}^{m} h_k^2 \to 0.$$

Under these conditions, as $n \to \infty$,

(i) $E\left(\widehat{f}(\omega)\right) \to f(\omega)$

(ii) $\left(\sum_{k=-m}^{m} h_k^2\right)^{-1} \operatorname{cov}\left(\widehat{f}(\omega), \widehat{f}(\lambda)\right) \to f^2(\omega) \quad \text{for } \omega = \lambda \neq 0, 1/2.$

In (ii), replace $f^2(\omega)$ by 0 if $\omega \neq \lambda$ and by $2f^2(\omega)$ if $\omega = \lambda = 0$ or $1/2$.

We have already seen these results in the case of $\bar{f}(\omega)$, where the weights are constant, $h_k = L^{-1}$, in which case $\sum_{k=-m}^{m} h_k^2 = L^{-1}$. The distributional properties of (4.56) are more difficult now because $\widehat{f}(\omega)$ is a weighted linear combination of asymptotically independent χ^2 random variables. An approximation that seems to work well is to replace L by $\left(\sum_{k=-m}^{m} h_k^2\right)^{-1}$. That is, define

$$L_h = \left(\sum_{k=-m}^{m} h_k^2\right)^{-1} \tag{4.57}$$

and use the approximation[13]

$$\frac{2L_h\widehat{f}(\omega)}{f(\omega)} \dot{\sim} \chi^2_{2L_h}. \tag{4.58}$$

In analogy to (4.48), we will define the bandwidth in this case to be

$$B_w = \frac{L_h}{n}. \tag{4.59}$$

Using the approximation (4.58) we obtain an approximate $100(1-\alpha)\%$ confidence interval of the form

$$\frac{2L_h\widehat{f}(\omega)}{\chi^2_{2L_h}(1-\alpha/2)} \leq f(\omega) \leq \frac{2L_h\widehat{f}(\omega)}{\chi^2_{2L_h}(\alpha/2)} \tag{4.60}$$

for the true spectrum, $f(\omega)$. If the data are padded to n', then replace $2L_h$ in (4.60) with $df = 2L_h n/n'$ as in (4.52).

An easy way to generate the weights in R is by repeated use of the Daniell kernel. For example, with $m = 1$ and $L = 2m + 1 = 3$, the Daniell kernel has weights $\{h_k\} = \{\frac{1}{3}, \frac{1}{3}, \frac{1}{3}\}$; applying this kernel to a sequence of numbers, $\{u_t\}$, produces

$$\widehat{u}_t = \tfrac{1}{3}u_{t-1} + \tfrac{1}{3}u_t + \tfrac{1}{3}u_{t+1}.$$

We can apply the same kernel again to the $\widehat{u}_t$,

$$\widehat{\widehat{u}}_t = \tfrac{1}{3}\widehat{u}_{t-1} + \tfrac{1}{3}\widehat{u}_t + \tfrac{1}{3}\widehat{u}_{t+1},$$

which simplifies to

$$\widehat{\widehat{u}}_t = \tfrac{1}{9}u_{t-2} + \tfrac{2}{9}u_{t-1} + \tfrac{3}{9}u_t + \tfrac{2}{9}u_{t+1} + \tfrac{1}{9}u_{t+2}.$$

The modified Daniell kernel puts half weights at the end points, so with $m = 1$ the weights are $\{h_k\} = \{\frac{1}{4}, \frac{2}{4}, \frac{1}{4}\}$ and

$$\widehat{u}_t = \tfrac{1}{4}u_{t-1} + \tfrac{1}{2}u_t + \tfrac{1}{4}u_{t+1}.$$

Applying the same kernel again to $\widehat{u}_t$ yields

$$\widehat{\widehat{u}}_t = \tfrac{1}{16}u_{t-2} + \tfrac{4}{16}u_{t-1} + \tfrac{6}{16}u_t + \tfrac{4}{16}u_{t+1} + \tfrac{1}{16}u_{t+2}.$$

Example 4.13 Smoothed Periodogram for SOI and Recruitment

In this example, we estimate the spectra of the SOI and Recruitment series using the smoothed periodogram estimate in (4.56). We used a modified Daniell kernel twice, with $m = 3$ both times. This yields $L_h = 1/\sum_{k=-m}^{m} h_k^2 = 9.232$, which is close to the value of $L = 9$ used in Example 4.11. In this case, the bandwidth is $B_w = 9.232/480 = .019$ and the modified degrees of freedom is $df = 2L_h 453/480 = 17.43$.

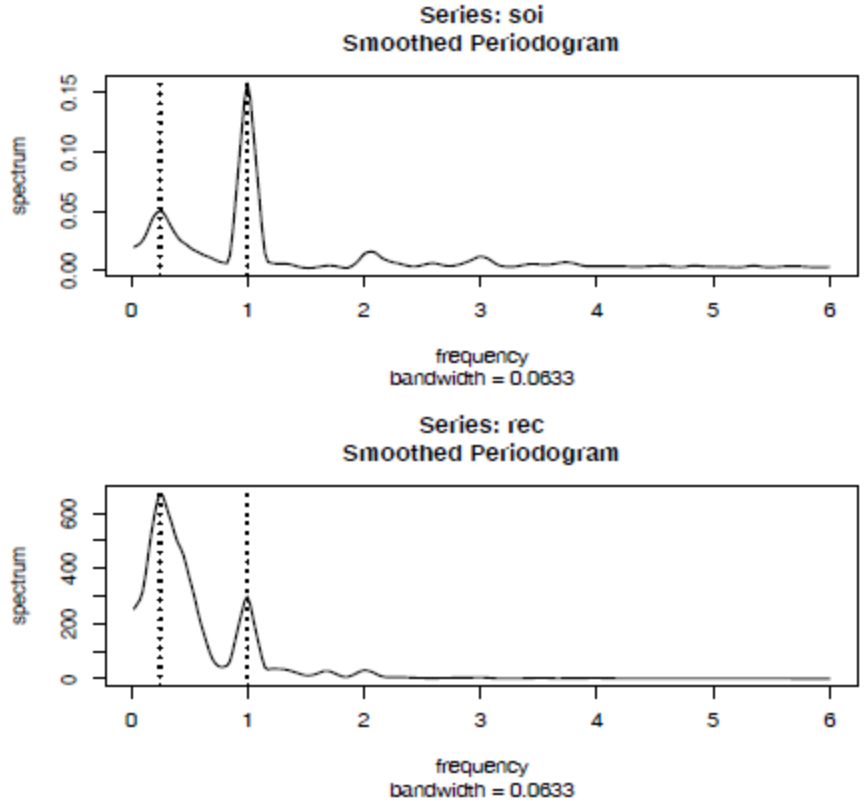

Fig. 4.8. Smoothed spectral estimates of the SOI and Recruitment series; see Example 4.13 for details.

We are now ready to briefly introduce the concept of *tapering*; a more detailed discussion may be found in Bloomfield (2000, §9.5). Suppose x_t is a mean-zero, stationary process with spectral density $f_x(\omega)$. If we replace the original series by the tapered series

$$y_t = h_t x_t, \tag{4.61}$$

for $t = 1, 2, \ldots, n$, use the modified DFT

$$d_y(\omega_j) = n^{-1/2} \sum_{t=1}^{n} h_t x_t e^{-2\pi i \omega_j t}, \tag{4.62}$$

and let $I_y(\omega_j) = |d_y(\omega_j)|^2$, we obtain (see Problem 4.15)

$$E[I_y(\omega_j)] = \int_{-1/2}^{1/2} W_n(\omega_j - \omega)\ f_x(\omega)\ d\omega \tag{4.63}$$

where

$$W_n(\omega) = |H_n(\omega)|^2 \tag{4.64}$$

and

$$H_n(\omega) = n^{-1/2} \sum_{t=1}^{n} h_t \mathrm{e}^{-2\pi i \omega t}. \tag{4.65}$$

The value $W_n(\omega)$ is called a spectral window because, in view of (4.63), it is determining which part of the spectral density $f_x(\omega)$ is being "seen" by the estimator $I_y(\omega_j)$ on average. In the case that $h_t = 1$ for all t, $I_y(\omega_j) = I_x(\omega_j)$ is simply the periodogram of the data and the window is

$$W_n(\omega) = \frac{\sin^2(n\pi\omega)}{n \sin^2(\pi\omega)} \tag{4.66}$$

with $W_n(0) = n$, which is known as the Fejér or modified Bartlett kernel. If we consider the averaged periodogram in (4.46), namely

$$\bar{f}_x(\omega) = \frac{1}{L} \sum_{k=-m}^{m} I_x(\omega_j + k/n),$$

the window, $W_n(\omega)$, in (4.63) will take the form

$$W_n(\omega) = \frac{1}{nL} \sum_{k=-m}^{m} \frac{\sin^2[n\pi(\omega + k/n)]}{\sin^2[\pi(\omega + k/n)]}\,. \tag{4.67}$$

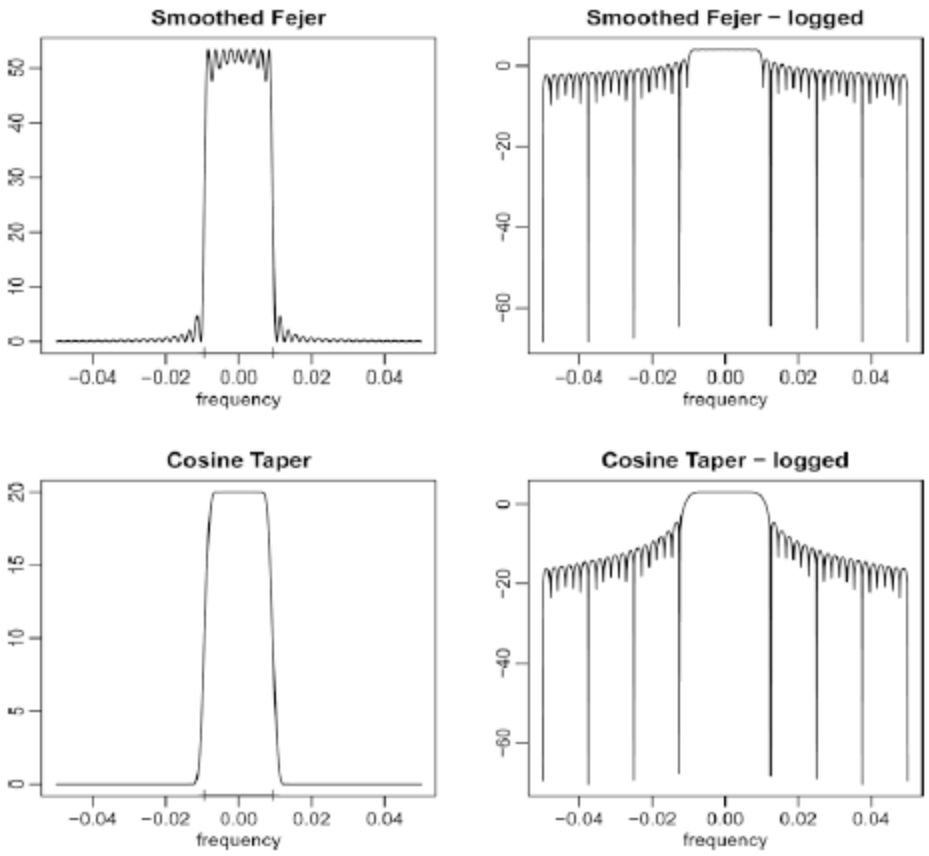

Fig. 4.9. Averaged Fejér window (top row) and the corresponding cosine taper window (bottom row) for $L = 9,\ n = 480$. The extra tic marks on the horizontal axis of the left-hand plots exhibit the predicted bandwidth, $B_w = 9/480 = .01875$.

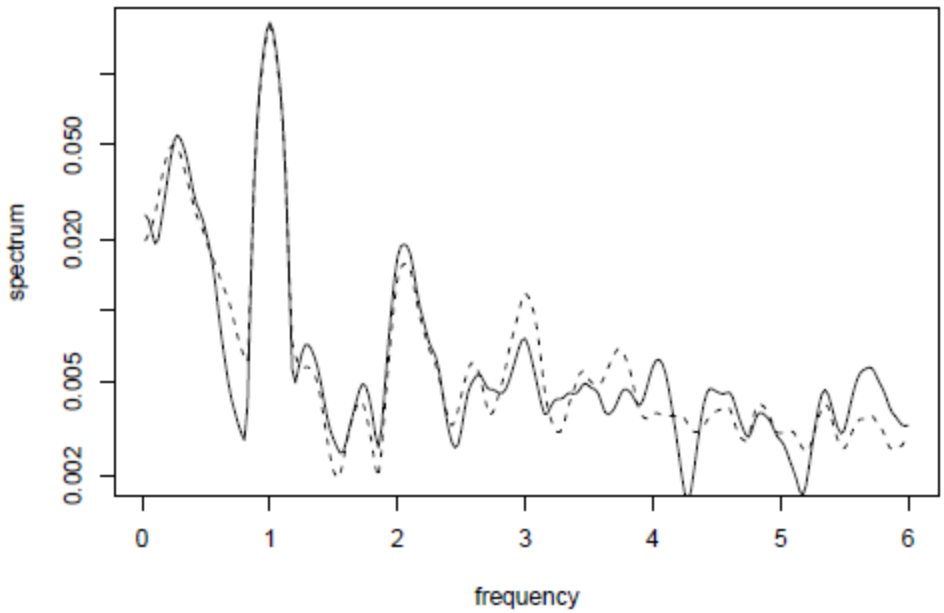

Fig. 4.10. Smoothed spectral estimates of the SOI without tapering (dashed line) and with full tapering (solid line); see Example 4.14 for details.

We close this section with a brief discussion of lag window estimators. First, consider the periodogram, $I(\omega_j)$, which was shown in (4.22) to be

$$I(\omega_j) = \sum_{|h|<n} \widehat{\gamma}(h) e^{-2\pi i \omega_j h}.$$

Thus, (4.56) can be written as

$$\begin{aligned} \widehat{f}(\omega) &= \sum_{|k|\le m} h_k \, I(\omega_j + k/n) \\ &= \sum_{|k|\le m} h_k \sum_{|h|<n} \widehat{\gamma}(h) e^{-2\pi i(\omega_j + k/n)h} \\ &= \sum_{|h|<n} g(h/n)\, \widehat{\gamma}(h) e^{-2\pi i \omega_j h}. \end{aligned} \tag{4.69}$$

where $g(h/n) = \sum_{|k|\le m} h_k \exp(-2\pi i k h/n)$. Equation (4.69) suggests estimators of the form

$$\widetilde{f}(\omega) = \sum_{|h|\le r} w(h/r)\ \widehat{\gamma}(h) e^{-2\pi i \omega h} \tag{4.70}$$

where $w(\cdot)$ is a weight function, called the lag window, that satisfies

(i) $w(0) = 1$
(ii) $|w(x)| \leq 1$ and $w(x) = 0$ for $|x| > 1$,
(iii) $w(x) = w(-x)$.

Note that if $w(x) = 1$ for $|x| < 1$ and $r = n$, then $\widetilde{f}(\omega_j) = I(\omega_j)$, the periodogram. This result indicates the problem with the periodogram as an estimator of the spectral density is that it gives too much weight to the values of $\widehat{\gamma}(h)$ when h is large, and hence is unreliable [e.g, there is only one pair of observations used in the estimate $\widehat{\gamma}(n-1)$, and so on]. The smoothing window is defined to be

$$W(\omega) = \sum_{h=-r}^{r} w(h/r)e^{-2\pi i\omega h}, \tag{4.71}$$

and it determines which part of the periodogram will be used to form the estimate of $f(\omega)$. The asymptotic theory for $\widehat{f}(\omega)$ holds for $\widetilde{f}(\omega)$ under the same conditions and provided $r \to \infty$ as $n \to \infty$ but with $r/n \to 0$. We have

$$E\{\widetilde{f}(\omega)\} \to f(\omega), \tag{4.72}$$

$$\frac{n}{r}\text{cov}\left(\widetilde{f}(\omega), \widetilde{f}(\lambda)\right) \to f^2(\omega)\int_{-1}^{1} w^2(x)dx \qquad \omega = \lambda \neq 0, 1/2. \tag{4.73}$$

In (4.73), replace $f^2(\omega)$ by 0 if $\omega \neq \lambda$ and by $2f^2(\omega)$ if $\omega = \lambda = 0$ or $1/2$.

Many authors have developed various windows and Brillinger (2001, Ch 3) and Brockwell and Davis (1991, Ch 10) are good sources of detailed information on this topic. We mention a few.

The rectangular lag window, which gives uniform weight in (4.70),

$$w(x) = 1, \quad |x| \leq 1,$$

corresponds to the Dirichlet smoothing window given by

$$W(\omega) = \frac{\sin(2\pi r + \pi)\omega}{\sin(\pi\omega)}. \tag{4.74}$$

$$\text{var}\{\widetilde{f}(\omega)\} \approx \frac{2r}{n}f^2(\omega).$$

The Parzen lag window is defined to be

$$w(x) = \begin{cases} 1 - 6x + 6|x|^3 & |x| < 1/2, \\ 2(1 - |x|)^3 & 1/2 \leq x \leq 1, \\ 0 & \text{otherwise.} \end{cases}$$

This leads to an approximate smoothing window of

$$W(\omega) = \frac{6}{\pi r^3} \frac{\sin^4(r\omega/4)}{\sin^4(\omega/2)}.$$

For large n, the variance of the estimator is approximately

$$\text{var}\{\widetilde{f}(\omega)\} \approx .539 f^2(\omega)/n.$$

The Tukey-Hanning lag window has the form

$$w(x) = \frac{1}{2}(1 + \cos(x)), \quad |x| \leq 1$$

which leads to the smoothing window

$$W(\omega) = \frac{1}{4} D_r(2\pi\omega - \pi/r) + \frac{1}{2} D_r(2\pi\omega) + \frac{1}{4} D_r(2\pi\omega + \pi/r)$$

where $D_r(\omega)$ is the Dirichlet kernel in (4.74). The approximate large sample variance of the estimator is

$$\text{var}\{\widetilde{f}(\omega)\} \approx \frac{3r}{4n} f^2(\omega).$$

The triangular lag window, also known as the Bartlett or Fejér window, given by

$$w(x) = 1 - |x|, \quad |x| \leq 1$$

leads to the Fejér smoothing window:

$$W(\omega) = \frac{\sin^2(\pi r\omega)}{r \sin^2(\pi\omega)}.$$

In this case, (4.73) yields

$$\text{var}\{\widetilde{f}(\omega)\} \approx \frac{2r}{3n} f^2(\omega).$$

The idealized rectangular smoothing window, also called the Daniell window, is given by

$$W(\omega) = \begin{cases} r & |\omega| \le 1/2r, \\ 0 & \text{otherwise}, \end{cases}$$

and leads to the sinc lag window, namely

$$w(x) = \frac{\sin(\pi x)}{\pi x}, \quad |x| \le 1.$$

From (4.73) we have

$$\text{var}\{\widetilde{f}(\omega)\} \approx \frac{r}{n} f^2(\omega).$$

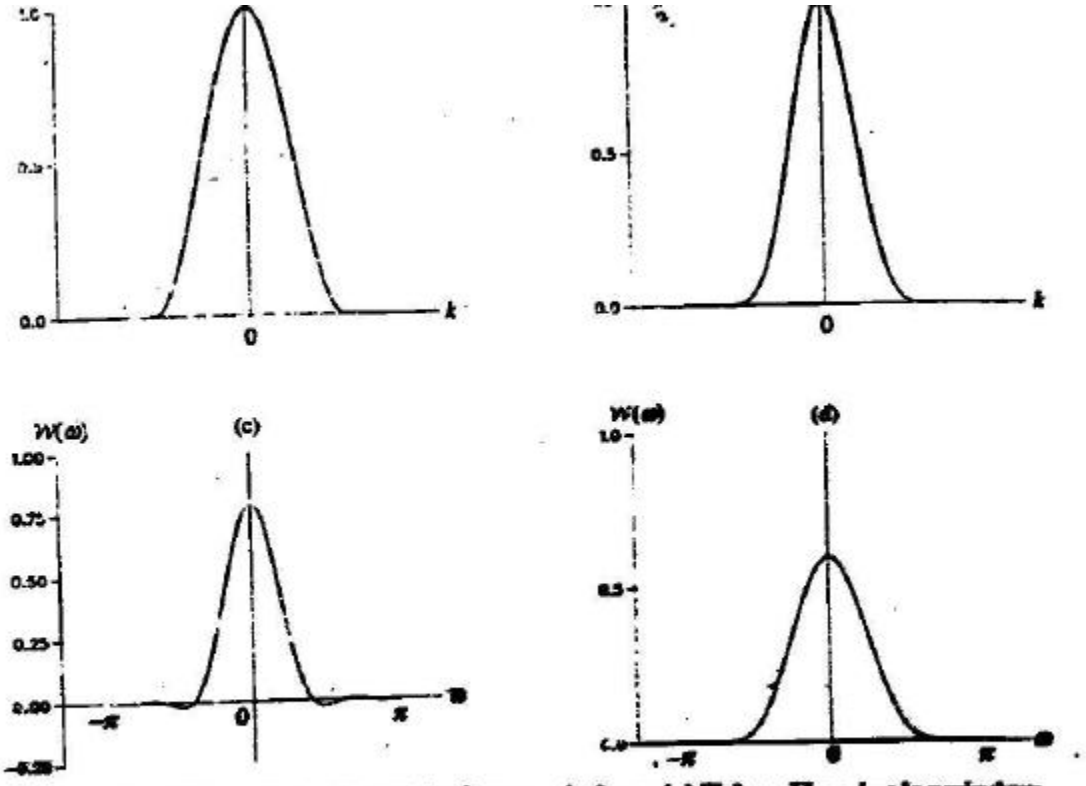

Fig. 12.6 The Tukey–Hanning and the Parzen windows. (a) Tukey–Hanning lag window ($M = 5$); (b) Parzen lag window ($M = 5$); (c) Tukey–Hanning spectral window ($M = 5$); (d) Parzen spectral window ($M = 5$).

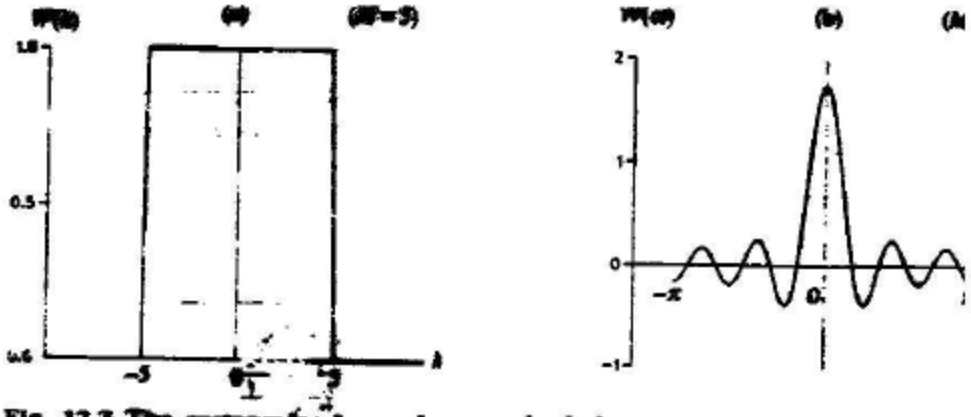

Fig. 12.3 The rectangular lag and spectral windows. (a) Rectangular lag win (b) Rectangular spectral window.

For lag window estimators, the width of the idealized rectangular window that leads to the same asymptotic variance as a given lag window estimator is sometimes called the equivalent bandwidth. For example, the bandwidth of the idealized rectangular window is $b_r = 1/r$ and the asymptotic variance is $\frac{1}{nb_r} f^2$. The asymptotic variance of the triangular window is $\frac{2r}{3n} f^2$, so setting $\frac{1}{nb_r} f^2 = \frac{2r}{3n} f^2$ and solving we get $b_r = 3/2r$ as the equivalent bandwidth.

Exemplo 8.3. A Figura 8.4 mostra os estimadores suavizados obtidos para as séries de marés de Ubatuba e de chuvas de Fortaleza, calculados usando o SPlus. Compare com os gráficos correspondentes das figuras 8.1 e 8.2. Na Figura 8.5 mostramos o estimador suavizado para a série de Fortaleza, na escala decibel, com o intervalo de confiança indicado à direita, no gráfico. A legenda da figura mostra a largura de faixa (*bandwidth*) usada para o cálculo do estimador e do intervalo de confiança.

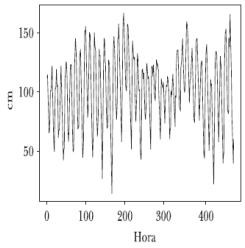

Figura 1.1: Dados horários da série de nível do mar obtidos em Ubatuba, SP.

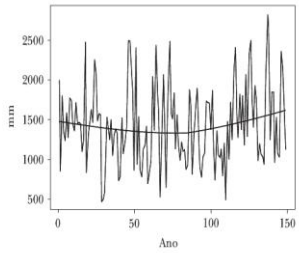

Figura 1.11: Série de precipitações de Fortaleza, Ceará, com curva ajustada pelo *Lowess*.

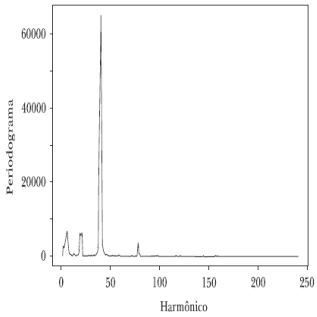

Figura 8.1: Periodograma da série de marés de Ubatuba.

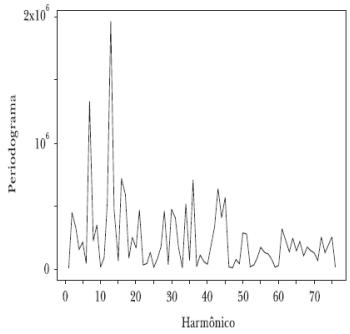

Figura 8.2: Periodograma da série de chuvas de Fortaleza.

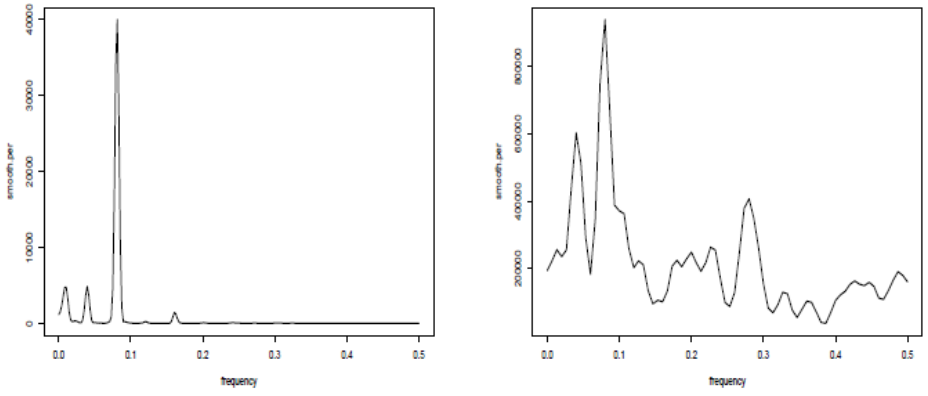

(a) (b)

Figure 8.4: Estimadores espectrais suavizados:
(a) Série de marés (Ubatuba); (b) Série de chuvas (Fortaleza).

Exemplo 8.4. Na Figura 8.6, temos o periodograma e um estimador suavizado para a série de sono-vigília da Figura 1.11. Vemos que em ambos há um pico correspondendo a um período de 24 horas. No periodograma, notamos a presença de dois outros picos, correspondentes a períodos de 12 e 8 horas, respectivamente.

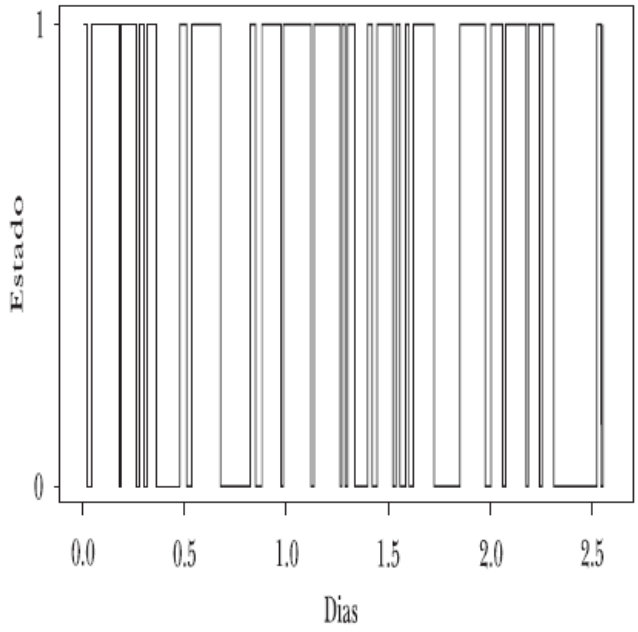

Figura 1.13: Série de sono-vigília de menino.

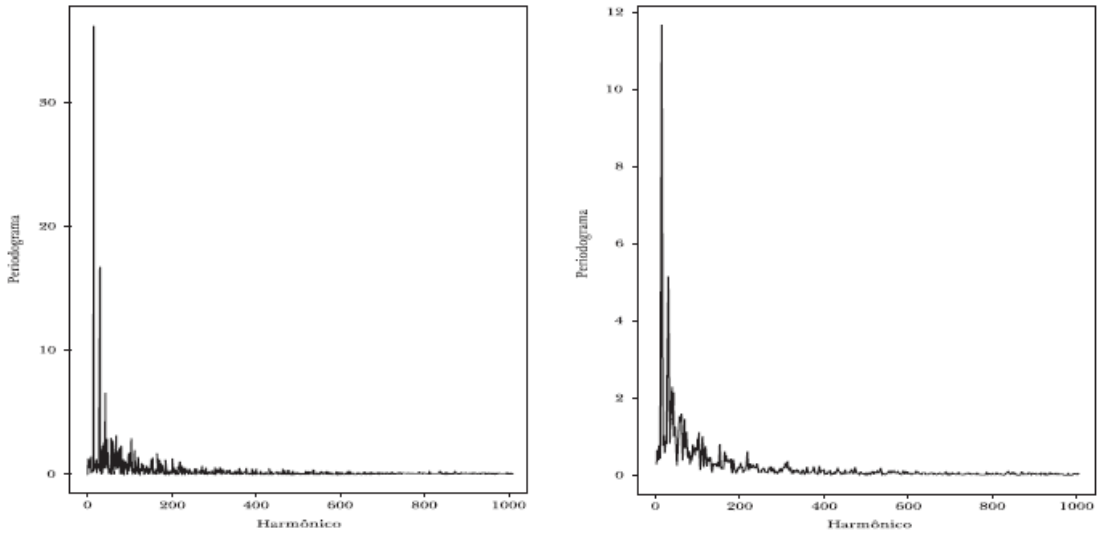

(a) (b)

Figura 8.6: Série de sono-vigília de um menino.
(a) Periodograma; (b) Estimador suavizado.

Exemplo 8.5. Considere a série de manchas solares de Wölfer, do exemplo 1.2 e Figura 1.7. Na Figura 8.7, temos o periodograma e um estimador suavizado dessa série, mostrando o período aproximado de 11 anos

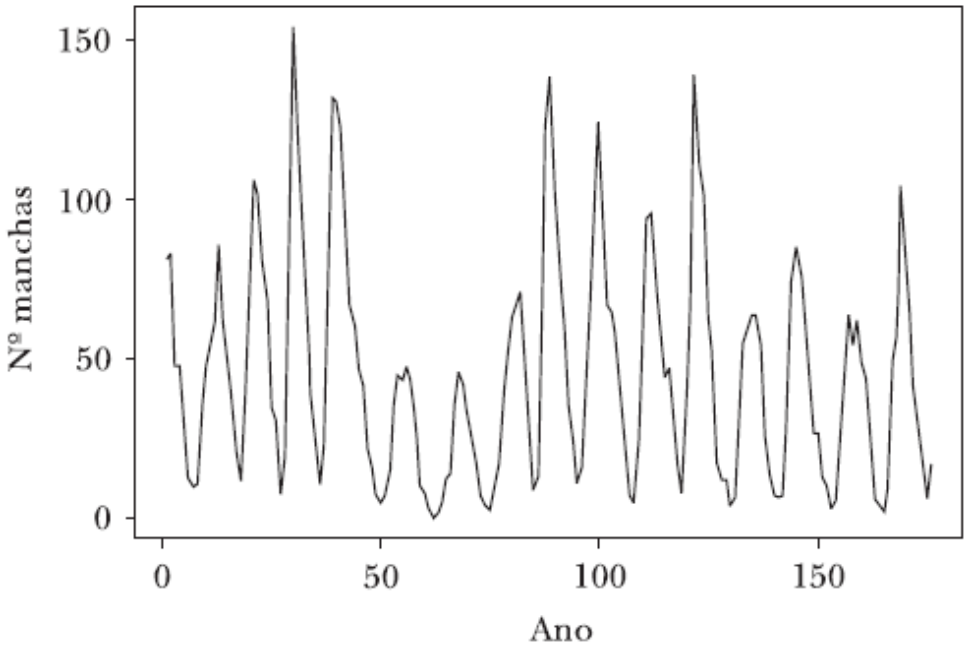

Figura 1.9: Série de manchas solares de Wölfer.

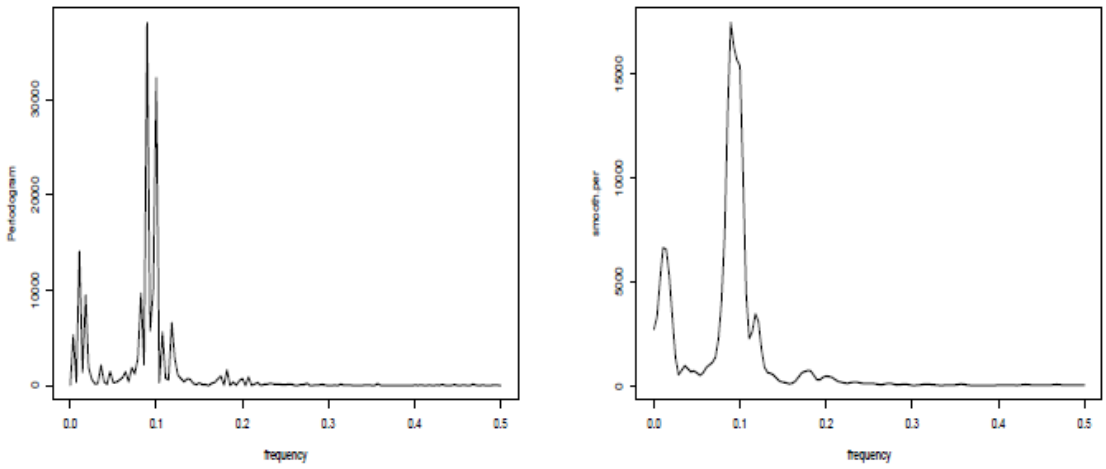

(a) (b)

Figura 8.7: Série de manchas solares de Wölfer.
(a) Periodograma; (b) Estimador suavizado.

4.6 Parametric Spectral Estimation

The methods of §4.5 lead to estimators generally referred to as nonparametric spectra because no assumption is made about the parametric form of the spectral density. In Property 4.3, we exhibited the spectrum of an ARMA process and we might consider basing a spectral estimator on this function, substituting the parameter estimates from an ARMA(p, q) fit on the data into the formula for the spectral density $f_x(\omega)$ given in (4.15). Such an estimator is called a parametric spectral estimator. For convenience, a parametric spectral estimator is obtained by fitting an AR(p) to the data, where the order p is determined by one of the model selection criteria, such as AIC, AICc, and BIC, defined in (2.19)-(2.21). Parametric autoregressive spectral estimators will often have superior resolution in problems when several closely spaced narrow spectral peaks are present and are preferred by engineers for a broad variety of problems (see Kay, 1988). The development of autoregressive spectral estimators has been summarized by Parzen (1983).

If $\widehat{\phi}_1, \widehat{\phi}_2, \ldots, \widehat{\phi}_p$ and $\widehat{\sigma}_w^2$ are the estimates from an AR(p) fit to x_t, then based on Property 4.3, a parametric spectral estimate of $f_x(\omega)$ is attained by substituting these estimates into (4.15), that is,

$$\widehat{f}_x(\omega) = \frac{\widehat{\sigma}_w^2}{|\widehat{\phi}(\mathrm{e}^{-2\pi i\omega})|^2}, \tag{4.75}$$

where

$$\widehat{\phi}(z) = 1 - \widehat{\phi}_1 z - \widehat{\phi}_2 z^2 - \cdots - \widehat{\phi}_p z^p. \tag{4.76}$$

The asymptotic distribution of the autoregressive spectral estimator has been obtained by Berk (1974) under the conditions $p \to \infty$, $p^3/n \to 0$ as $p,\ n \to \infty$, which may be too severe for most applications. The limiting results imply a confidence interval of the form

$$\frac{\widehat{f}_x(\omega)}{(1 + Cz_{\alpha/2})} \le f_x(\omega) \le \frac{\widehat{f}_x(\omega)}{(1 - Cz_{\alpha/2})}, \tag{4.77}$$

where $C = \sqrt{2p/n}$ and $z_{\alpha/2}$ is the ordinate corresponding to the upper $\alpha/2$ probability of the standard normal distribution. If the sampling distribution is to be checked, we suggest applying the bootstrap estimator to get the sampling distribution of $\widehat{f}_x(\omega)$ using a procedure similar to the one used for $p = 1$ in

Example 3.35. An alternative for higher order autoregressive series is to put the AR(p) in state-space form and use the bootstrap procedure discussed in §6.7.

Property 4.5 AR Spectral Approximation

Let $g(\omega)$ be the spectral density of a stationary process. Then, given $\epsilon > 0$, there is a time series with the representation

$$x_t = \sum_{k=1}^{p} \phi_k x_{t-k} + w_t$$

where w_t is white noise with variance σ_w^2, such that

$$|f_x(\omega) - g(\omega)| < \epsilon \quad \text{forall } \omega \in [-1/2, 1/2].$$

Moreover, p is finite and the roots of $\phi(z) = 1 - \sum_{k=1}^{p} \phi_k z^k$ are outside the unit circle.

Example 4.15 Autoregressive Spectral Estimator for SOI

Consider obtaining results comparable to the nonparametric estimators shown in Figure 4.5 for the SOI series. Fitting successively higher order AR(p) models for $p = 1, 2, \ldots, 30$ yields a minimum BIC at $p = 15$ and a minimum AIC at $p = 16$, as shown in Figure 4.11. We can see from Figure 4.11 that BIC is very definite about which model it chooses; that is, the minimum BIC is very distinct. On the other hand, it is not clear what is going to happen with AIC; that is, the minimum is not so clear, and there is some concern that AIC will start decreasing after $p = 30$. Minimum AICc selects the $p = 15$ model, but suffers from the same uncertainty as AIC. The spectra of the two cases are almost identical, as shown in Figure 4.12,

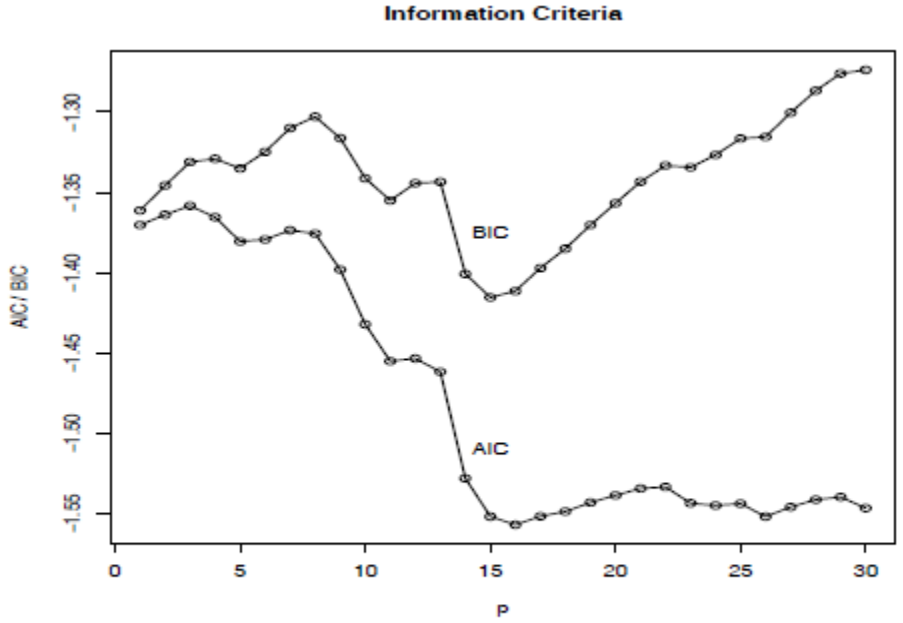

Fig. 4.11. Model selection criteria AIC and BIC as a function of order p for autoregressive models fitted to the SOI series.

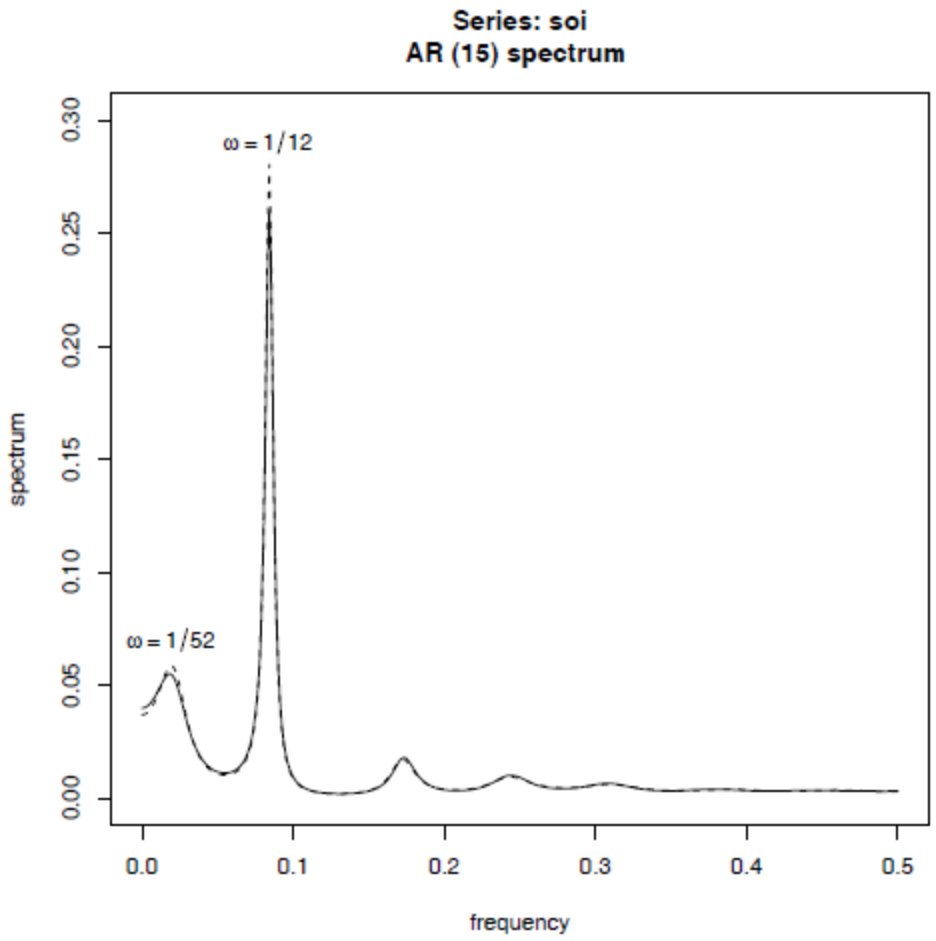

Fig. 4.12. Autoregressive spectral estimators for the SOI series using models selected by AIC ($p = 16$, solid line) and by BIC and AICc ($p = 15$, dashed line). The first peak corresponds to the El Niño period of 52 months.